

COMPARISON OF ENVISAT ASAR OCEAN WAVE SPECTRA WITH BUOYS AND ALTIMETER OBSERVATIONS VIA A WAVE MODEL

Jian-Guo Li and Martin Holt

Met Office, FitzRoy Road, Exeter, EX1 3PB, United Kingdom

ABSTRACT

The Advanced Synthetic Aperture Radar (ASAR) on board the European Space Agency Envisat satellite is one of a few instruments which measures the directional characteristics of the ocean surface waves on a global scale and provides an unprecedented resource for ocean wave models. Assessment of the ASAR data quality is, however, difficult due to lack of independent observations of similar temporal and spatial scales. The ocean wave heights measured by the radar altimeter instrument (RA2) onboard the same satellite as the ASAR can only be used for partial validation of the ASAR data as they do not have any spectral and directional information, not to mention that the ASAR spectra are displaced from the RA2 measurements due to the slant beam of the ASAR instrument. Moored ocean data buoys are another independent observation and some of them offer wave spectral and directional information though their spatial coverage is very limited. Direct comparison of ASAR data with buoy observations is not practical as few ASAR spectra fell on the exact position of any buoy, prohibiting any meaningful statistical application. An indirect comparison of these three independent observations is made possible by an intermediate wave model, which provides coherent links to fill the time and space gaps among these observations. Eighteen-month (July 2004 - Dec 2005) satellite and buoy data are used for this comparison. Wave spectra are integrated as total and 4-sub range wave heights for comparison. This spectral breakdown of ocean wave energy sheds some light on the spectral characteristics of these ocean wave data. Results indicate that the ASAR performance is better in the open ocean than near coastlines and ASAR wave height is generally in agreement with other two independent observations.

1 INTRODUCTION

The Advanced Synthetic Aperture Radar (ASAR) on board the European Space Agency Envisat satellite is one of a few instruments which can measure the directional characteristics of the ocean wave field on a global scale [1] and provide an unprecedented resource for ocean wave models. Assessment of the ASAR data quality is, however, difficult due to lack of independent observations of similar temporal and spatial scales. The ocean wave heights measured by the radar altimeter instrument (RA2) onboard the same satellite as the ASAR are of similar spatial coverage but can only be used for total wave energy validation of integrated ASAR data as they do not have any spectral and directional information, not to mention that the ASAR spectra are displaced from the RA2 measurements due to the slant beam of the ASAR instrument. Moored ocean data buoys are another independent observation and some of them offer temporally continuous wave spectral and directional information on fixed ocean sites [2]. The number of buoys is, however, very limited and they are not evenly distributed in the ocean. Most of them are located near coastal lines and very few in deep waters.

It is envisaged that direct comparison of satellite data with buoy ones would lead to few data pairs within the 18-month period (July 2004 – Dec 2005), prohibiting any meaningful statistical application. The Met Office wave model [3] is then used as an intermediate medium for the satellite and buoy data comparison and it provides coherent links to fill the time and space gaps among these observations. The performance of this wave model is comparable to other operational wave models, such as the 3rd generation WAM model [4].

2 THE MET OFFICE WAVE MODEL

The Met Office operational wave model was developed in the 70's [3] and continuously modified by subsequent development [5]. The wave model is based on the 2-D spectral wave energy equation given by

$$\frac{\partial E}{\partial t} + \nabla \cdot (E \mathbf{c}_g) + \frac{\partial}{\partial \theta} (E \mathbf{c}_g \cdot \nabla \theta) = S(f, \theta, x, y, t) \quad (1)$$

where f = wave spectral frequency (Hz); θ = wave spectral direction (rad); x, y = horizontal space coordinates (m); $\nabla \equiv \mathbf{i} \partial / \partial x + \mathbf{j} \partial / \partial y$ the horizontal gradient operator; t = time (s); $E(f, \theta, x, y, t)$ = wave spectral energy ($\text{m}^2 \text{Hz}^{-1} \text{rad}^{-1}$);

$S(f, \theta, x, y, t)$ = the source term; and c_g = the wave spectral group velocity (m s^{-1}). The operational wave spectral model suite run in the Met Office provides analyses and forecasts of sea state on grid spacing of approximately 60 km for the global model and 12 km for the nested regional models. As standard the models operate with a spectral resolution of 13 frequency bands from approximately 0.04 to 0.4 Hz and 16 directional bins, which represents waves with a range of periods between 3 and 25 seconds. The wave model is forced by hourly winds at 10m above mean sea-level generated in the Met Office Unified Model, which include observations from satellite, ship and data buoy networks in their 4-DVar assimilation schemes. For integrated parameters (such as total wave energy) the overall performance of the Met Office wave model is comparable to other operational wave models [6].

The 2-D ocean wave energy spectrum $E(f, \theta)$ (here the spatial and time variables are omitted for simplicity) is integrated to yield the significant wave height (SWH), H_s , in unit of m, within a given frequency range (f_1, f_2) defined by

$$H_s(f_2 - f_1) = 4 \left(\int_{f_1}^{f_2} df \int_0^{2\pi} d\theta \cdot E(f, \theta) \right)^{1/2} \quad (2)$$

The total SWH over the whole frequency range is then equal to $H_s(\infty - 0)$. Apart from comparison of the total SWH, wave energy in 4 frequency sub-ranges (see Fig.1) is also compared. This spectral breakdown of ocean wave energy sheds some light on the spectral characteristics of the ocean waves.

3 OBSERVATION DATA

The Envisat ASAR level 2 products we use are the ASA_WVW_2P series, obtained twice a day from the ESA ftp site. We also retrieve the Envisat RA2 altimeter ocean SWHs at the same time. Directional wave energy spectra of moored buoys are retrieved once a month from the (American) National Data Buoy Center (NDBC) web site (www.ndbc.noaa.gov). We select two buoys particularly for this study: one is near the Christmas Island (CI, Buoy ID 51028 at $0.02^\circ \text{ S } 153.87^\circ \text{ W}$) and another is in the Gulf of Mexico (GM, Buoy ID 42001 at $25.86^\circ \text{ N } 89.67^\circ \text{ W}$). The CI buoy is located in the middle of the Pacific Ocean where long distance swell is expected and wind speed is usually small in this region. So the CI buoy site is an ideal location to validate swell wave energy. The GM buoy is, in contrast, within enclosed water where long-distance swell is excluded by its natural boundary and only wind-sea is expected. So it is useful to test the high frequency wind sea wave spectral part. ASAR and RA2 data close to these two buoys in a 5 degree (latitude and longitude from the buoy site) box are collected for buoy-model-ASAR-RA2 inter-comparisons. ASAR and buoy wave spectra are also integrated for total and 4-bin SWH. The 4 spectral bins (4-bin) are defined roughly by the wave period bounds of 23, 16, 11, 8, and 5 s and rounded to the nearest frequency bands of each of the data set as showed in Fig.1 by the vertical bars in unit of frequency Hz. The frequency bands for the models, buoys and ASAR observations are showed by the black stars (band centre). The green arrows indicate the band margins.

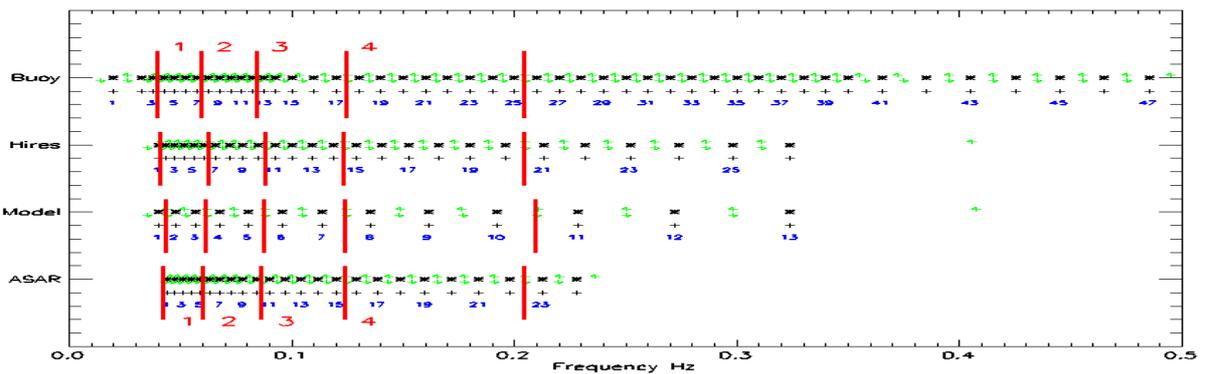


Fig.1. Definition of the 4 frequency bins for comparison of model and observed ocean wave energy spectra.

4 COMPARISON RESULTS

The comparison will be divided into 2 sections, starting with the total wave energy or SWH comparison and then the 4-bin SWH comparison.

4.1 Total Wave Energy Comparison

The top-left plot in Fig.2 is a scatter plot of the model and CI buoy total SWHs over 18 months from July 2004 to December 2005. Each pair of model and buoy SWHs are plotted as a green plus symbol in the diagram with its x-coordinate equal to the buoy SWH and y-coordinate to the model SWH. The contours indicate the data density and the large cross sign marks the model and buoy mean SWHs (cross centre). Standard deviations (SDs) of the model and buoy SWHs are indicated by the y- and x-size of the cross sign, respectively. There are 11068 pairs of data in the scatter plot. The mean value of the model total SWHs (2.21 m) at the buoy site is slightly higher than the average of the buoy SWHs (1.87 m). The model and buoy SDs are 0.381 m and 0.357 m, respectively. The SD or root-mean-square (rms) of the model and buoy SWH difference is 0.362 m. The correlation coefficient for the model and buoy data is 0.519. These results are comparable to those of another validation work [2] (Bidlot et al 2002).

The lower-left plot in Fig.2 compares the model SWHs with the RA2 altimeter data within 5 degree (latitudinal and longitudinal) distance from the CI buoy site during the same 18 months (July 2004 – December 2005) as the buoy plot. A total of 5356 pairs of data are selected here. Altimeter data at rain points are excluded as the data are less reliable at those points. The altimeter SWH is actually the average of all altimeter data (about 9 values) along the satellite track within the model grid box at which the model SWH is used. The model mean SWH (2.25 m) is slightly higher than the altimeter mean (2.07 m). The SDs of the model and RA2 SWHs are 0.379 and 0.386 m, respectively. The overall rms value of the model and RA2 SWH difference is 0.334 m and the correlation coefficient 0.620. So the RA2 SWHs are in agreement with the model values as the buoy ones.

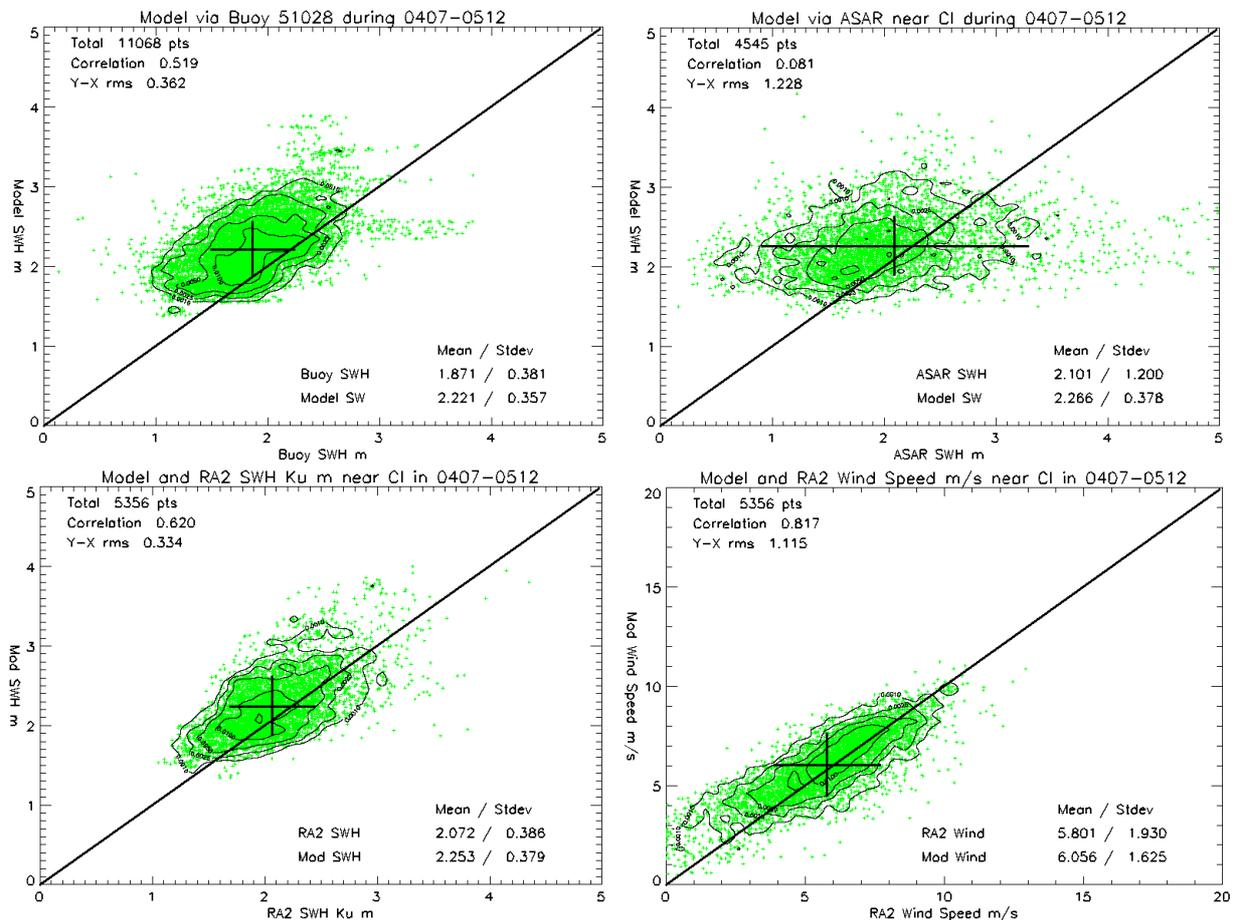


Fig.2. Comparison of model results with the CI buoy and Envisat measurements near the CI buoy site.

The top-right panel in Fig.2 is the scatter plot of model SWHs against ASAR level 2 SWHs within the same 5 degree distance from the CI buoy site and the same 18 months time interval as the RA2 plot. There are 4545 pairs of data in this selection, comparable to the RA2 case. The model mean SWH (2.27 m) and SD (0.378 m) are similar as those in the RA2 plot. This is expected as both plots used the model spectra along the same satellite tracks. The ASAR mean SWH (2.10 m)

is slightly lower than the model mean but ASAR SWHs show much larger variations than RA2 ones. The ASAR SD (1.20 m) is much larger than the model SD and the rms value of the model and ASAR SWH difference is 1.23 m, much higher than both the RA2 one (0.334 m) and the buoy one (0.362). The correlation between model and ASAR SWHs is very poor (0.081).

The lower-right plot in Fig.2 is a scatter plot of the model wind speeds against the measured wind speeds from the Envisat RA2 data. The wind speed pairs are selected using a similar criterion (5 degree distance in space and 18 months in time) as for the RA2 SWHs in the lower-left plot of Fig.2. The mean model wind speed (6.06 m s^{-1}) is slightly higher than the mean Envisat wind speed (5.80 m s^{-1}). Notice that the CI buoy site is at the middle of the Pacific Ocean and is under continuous influence of long-distance traveling swells from the broad Pacific Ocean. So the local winds near the buoy site contribute only to part of the total wave energy. This explains why the SWHs around the CI buoy are seldom below 1.5 m no matter that local wind speed is quite small sometime as shown in the wind speed scatter plot.

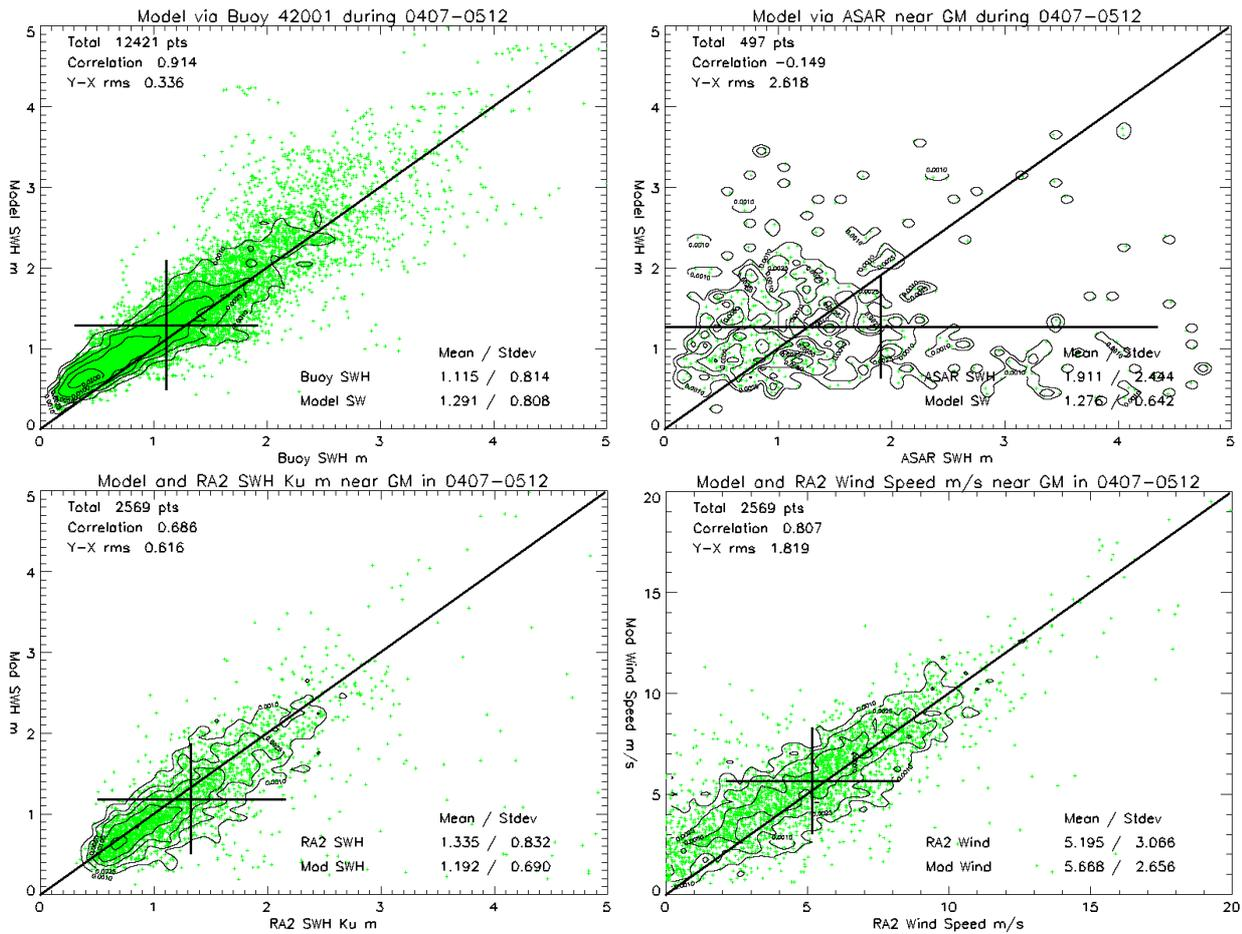


Fig.3 Comparison of model and observation near the GM buoy site

Fig.3 is similar to Fig.2 but for the GM buoy site. As the GM buoy site is inaccessible to most of ocean swells, wave energy at the GM site is dominated by locally-generated wind-sea, which is proportional to the local wind speed. So the SWH scatter plots for the GM buoy (top-left) and the RA2 altimeter (lower-left) are similar to that of the wind speed scatter plot (lower-right). The modeled SWHs are in good agreement with both the buoy and altimeter observations with rms SWH difference at 0.336 and 0.616 m, respectively. The correlation of model and observed SWH is quite good (0.914 for GM buoy and 0.686 for RA2 near GM) and is also better than those at the CI buoy site as showed in Fig.2 (0.519 for CI buoy and 0.620 for RA2 near CI), thanks to the increased SWH range at this site.

The ASAR SWHs (top-right), however, hardly show any correlation to the modeled values and the rms difference is quite large (2.62 m). There are two possible reasons for this poor ASAR performance. First, the Envisat track coverage over the GM buoy site is much scarce (497 pairs) in comparison with that over the CI buoy site (4545 pairs). The other possible cause is land effects, which usually results in erroneous large wave height. As Gulf of Mexico is relatively small and

surrounded by coastlines within the 5 degree box, the selected ASAR wave spectra may have been impaired by radar echoes from coastal land surface. The land effects also affect the altimeter data but the averaging procedure helps remove most of these large values. The effects are clearly showed by wave height plot along satellite tracks as most of the large 'wave heights' appear near coastlines.

4.2 Comparison of 4-bin Wave Energy

The 4-bin wave energy scatter plots of model against the CI and GM buoys are showed in Fig.4. These data are exactly the same as used in Fig.2 and Fig.3 except that they are integrated in the 4 sub-ranges showed in Fig.1. The first two bins (period 23-11 s) may be considered representing long-distance swells while the last two bins (period 11-5 s) are deemed to be the wind sea. At the CI buoy site (left two columns in Fig.4), where long-distance swells are expected, both the model and buoy wave spectra show relatively large sub-range SWHs in the first two bins (32-16 and 16-11 s plots) though the modeled swell energy is slightly higher than the buoy measurements. Swell energy at the GM buoy, as showed in the right two columns in Fig.4, is quite small in both the model and buoy measurements because the GM site is inaccessible to long-distance swells. Most of the wave energy at the GM buoy site is concentrated in the highest frequency (or shortest period 8-5 s) bin, which is purely wind sea contribution. The wave model generally performs well over the full frequency range, especially for wind sea at both buoy sites as indicated by the large correlation coefficients for the 8-5 s bin (0.761 for CI and 0.918 for GM). Model swell energy is slightly higher than the CI buoy measurement.

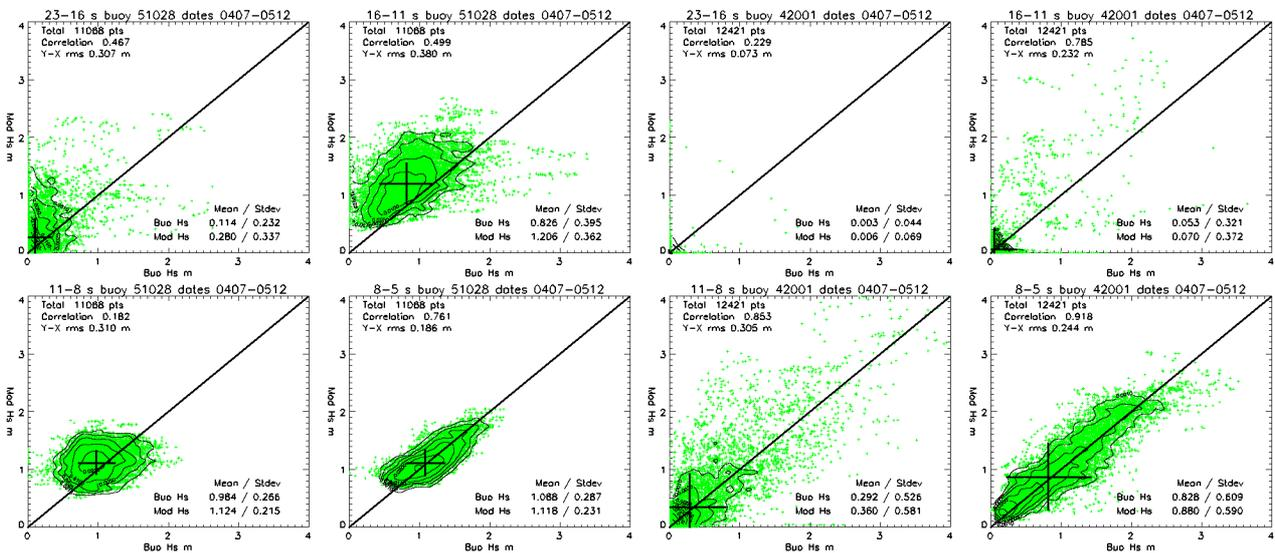


Fig.4. Comparison of model and CI (51028) and GM (42001) buoy wave spectra in 4 bins.

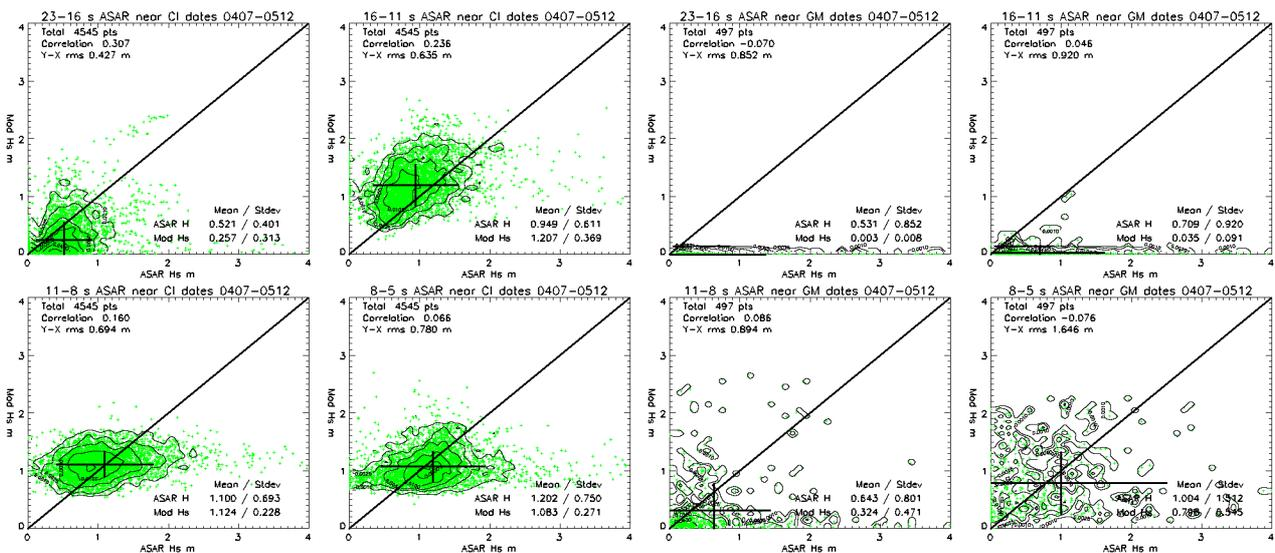


Fig.5. Comparison of model and Envisat ASAR 4-bin wave energy near the CI and GM buoy sites.

A 4-bin break down of the ASAR wave energy near the CI and GM buoy sites is also showed here in Fig.5. At the CI buoy site, ASAR performance is comparable to the buoy in all the 4 sub-ranges except the deviation is slightly larger than buoy one. In addition, the ASAR spectra over-estimated the long-period swell energy as showed by the first bin (23-16 s bin) at both buoy sites. This is even obvious at the GM buoy site as swell energy is expected to vanish there. In fact, both the GM buoy and model first bin mean SWH is below 0.01 m while the ASAR first bin mean SWH is over 0.5 m. At the CI buoy site model first bin mean SWH (0.26-0.28 m) is higher than CI buoy (0.11 m) but lower than ASAR (0.52 m). The other 3 (16-11 s, 11-8 s and 8-5 s) bins show quite good agreement between the ASAR and CI buoy while the wave model slightly over-estimates the second (16-11 s) bin energy. At the GM buoy site, the ASAR values are larger than the GM buoy measurement in all the 4 sub-ranges, implying that land effects are to be blamed.

5 SUMMARY AND CONCLUSIONS

Ocean wave energy observations from three independent sources: the buoy, the Envisat ASAR and RA2 altimeter, are compared via the intermediate Met Office global ocean wave model, which provides a coherent links over space and time among these observations. Comparison of the model total and 4 spectral sub-range wave heights with buoy, ASAR and RA2 data indicates that the wave model performs well over the full ocean wave frequency range, from long-period swells to high-frequency wind-sea. The results show that all the three observations are in good agreement in terms of total wave energy or SWH. The indirect comparison revealed that the Envisat ASAR level 2 wave spectra are comparable with buoy spectra in the open ocean, or more precisely, at the CI buoy site. Both altimeter and ASAR near shore wave energy may be impaired by coastal land surfaces and less reliable than open ocean ones. Besides, ASAR wave spectra generally over-estimate long ocean swells and have larger variations than buoy and model wave spectra.

Acknowledgement: We are very grateful to Dr Jim Gunson (Met Office) for providing programs for retrieval and processing of the ASAR and RA2 data and Dr Gary Fullerton (Met Office) for assistance in the wave model transfer to our new computer system. We would also like to thank Dr Jean Bidlot (ECMWF) for his suggestions about the NDBC buoy data.

6 REFERENCES

1. Hasselmann, S., Bruning, C., Hasselmann, K. and Heimbach, P.: An improved algorithm for the retrieval of ocean wave spectra from synthetic aperture radar image spectra. *J. Geophys. Res.* **101**, C7, 16615-16629, 1996.
2. Steele, K. E., Teng, C. C. and Wang, D. W. C.: Wave direction measurements using pitch and roll buoys. *Ocean Engineering*, **19**(4), 349-375, 1992.
3. Golding, B. W.: A wave prediction system for real-time sea state forecasting. *Q J Roy Met Soc.* **109**, 393-416, 1983.
4. WAMDI group: The WAM model - a third generation ocean wave prediction model. *J. Phys. Oceanogr.* **18**, 1775-1810, 1988.
5. Holt, M.: Improvement to UKMO wave model swell dissipation and performance in light winds. *Met Office Forecasting Research Division Tech. Rep.* **119**, 12pp, 1994.
6. Bidlot, J.R., Holmes, D. J., Wittmann, P. A., Lalbeharry, R and Chen, H. S.: Inter-comparison of the performance of operational ocean wave forecasting systems with buoy data. *Weather and Forecasting*, **17**, 287-310, 2002.